RSC Advances

ROYAL SOCIETY
OF CHEMISTRY

www.rsc.org/advances

Experimental and theoretical studies on the mechanism for chemical oxidation of multiwalled carbon nanotubes

B.M. Maciejewska*[1,2], M. Jasiurkowska-Delaporte*[1], A.I. Vasylenko[3], K.K. Kozioł[4],

S. Jurga[1,2]

[1]*NanoBioMedical Center, Adam Mickiewicz University, Umultowska 85, 61-614 Poznań, Poland*

[2]*Department of Macromolecular Physics, Faculty of Physics, Adam Mickiewicz University Umultowska 85, 61-614 Poznań, Poland*

[3]*Institute for Condensed Matter Physics, National Academy of Science of Ukraine, 1 Sventsitskogo Str., 79011 Lviv, Ukraine*

[4] *University of Cambridge, Department of Materials Science and Metallurgy, 27 Charles Babbage Road, Cambridge CB3 0FS, United Kingdom*

Abstract

In this study, the oxidation of multiwalled carbon nanotubes (MWCNTs) sonicated and/or refluxed in acids (H_2SO_4/HNO_3) was investigated using a combination of high-resolution transmission electron microscopy, Raman spectroscopy, Fourier transform infrared spectroscopy, and *ab initio* computational methods. Sonication of the sample has the strongest effect, leading to the highest concentration of defects and carboxyl groups on the walls. Substantial correlations between treatment protocols, CNT size, and the types of chemical moieties are observed. Finally, based on experimental and computational results, we suggest the mechanism of the oxidation process for attaching the functional groups on the sidewalls.

*Corresponding authors: Tel:48618295 239. Email: bmacieje@amu.edu.pl (Barbara Małgorzata Maciejewska), Tel:48618295 239. Email: maljas@amu.edu.pl (Małgorzata Jasiurkowska-Deporte)

1. Introduction

Owing to their remarkable physical properties, carbon nanotubes (CNTs) offer unique opportunities to fabricate advanced materials for various applications including drug delivery systems, biosensors, transistors, and nanocomposites [1-3]. The major challenges in achieving practical use of CNTs in biomedicine are enhancing their dispersibility in hydrophilic solvents and enhancing their chemical reactivity [2-4]. Chemical oxidation with acids damages the graphite-like structure, generates chemically active defects, and attaches various chemical groups [5]. The diversity and abundance of attached groups depend on the oxidation protocol and type of acid used [6,7]. Up to now, a few papers have presented *ab initio* studies of SWCNTs functionalized with covalently bonded COOH, NH_2, or $CONH_2$ on their sidewalls and tips [8-10], and the binding energies and the dependence of the physical properties of the SWCNTs (e.g., density of states) on the functionalization have been demonstrated. However, despite the experimental and theoretical research carried out so far, a clear understanding of the mechanism of CNT oxidation process remains elusive.

In this work, we investigate the influence of three different oxidation procedures on the outer walls of MWCNTs using high-resolution transmission electron microscopy (HR-TEM), Raman spectroscopy, Fourier transform infrared spectroscopy (FTIR), and *ab initio* computational methods using the density functional theory (DFT) approximation. The HR-TEM results illustrate the morphology of the sample, while the Raman spectra provide quantitative information about the degree of damage to the MWCNT walls. FTIR has the unique capacity to probe selected vibrations of molecular units, and DFT [11] is a powerful method for describing the properties of CNTs using first-principles calculations of the electronic structure [12,13]. Combining these experimental and computational results, we obtain a detailed picture of the impact of acid treatment on the MWCNT surface. We then present the correlations between the oxidation protocol, CNT size, degree of damage to the CNT, and types of functional groups.

2. Experimental details

2.1 Synthesis

All MWCNTs were synthesized using a floating-catalyst chemical vapour deposition method (CVD). MWCNTs with three different iron catalyst contributions were prepared: 2%-, 5%-, and 10%-MWCNTs. The different catalyst contents used in the synthesis resulted in various

diameter ranges and qualities of the obtained carbon nanostructures. Three different functionalization protocols were examined for the 2%-, 5%-, and 10%-MWCNTs, as follows:

> **Protocol I: Sonication treatment**. The 2%-, 5%-, and 10%-MWCNTs were dispersed in a mixture of sulphuric and nitric acid, and the resulting suspension was placed in an ultrasound bath with a controlled temperature (>50°C) for 24 hours. This treatment placed focused mechanical stress on the sample due to its contraction and expansion.

> **Protocol II: Reflux treatment**. The 2%-, 5%-, and 10%-MWCNTs were dispersed in a mixture of sulphuric and nitric acid and refluxed in a round-bottom flask attached to a condenser for 15 minutes at a temperature of 120°C. To explore the effect of the reflux time, the 5% sample was further treated for 25 and 35 minutes.

> **Protocol III: Sonication + reflux treatment**. The 2%-, 5%-, and 10%-MWCNTs were dispersed in a mixture of sulphuric and nitric acid. Then, the sonication (3 h, >50°C) and reflux (15 min, 120°C) methods were both applied.

The oxidised MWCNTs (O-MWCNTs) were then separated according to their length by centrifugation. The statistic of length distribution revealed that the O-MWCNT length is in the range from 1,2µm to 0,3µm.

2.2 Experimental techniques

The HR-TEM images were obtained with a Jeol ARM 200F HRTEM. The Raman spectra were obtained using a Ramascope-1000 spectrometer. The excitation source was a He-Ne laser (λ=633nm). Each spectrum was collected with four accumulations of 10 s. FTIR absorption spectra were measured using a BRUKER IFS 66/s spectrometer in the wavenumber range of 1000 cm^{-1} to 4000 cm^{-1} with a resolution of 4 cm^{-1}. Prior to the measurements, the MWCNTs were mixed with 0.2 g of potassium bromide (KBr) then compressed into a thin pellet. There is no chemical interaction between functional groups attached to the outer walls of the MWCNTs and the KBr.

3. Computational methods

All calculations were based on density functional theory (DFT). Most of them were performed using the Gaussian 09 program [14] with the B3LYP exchange-correlation density functional [15-17] and the 6-31G(d,p) basis set. However, the calculations of the cohesion energy of the SWCNTs and the energies for breaking the bonds between the carbon atoms

were performed with the ABINIT package, which implements the plane-wave approximation [18,19]. The full relaxation and geometry optimization of each system was performed for every considered case: pristine SWCNTs, SWCNTs with a reconstructed surface, and SWCNTs with functional groups attached. The functionalization of the surface of an external wall of a MWCNT is believed proceed in a similar way to the functionalization of a SWCNT. In order to reduce the computational costs and enable *ab initio* simulations of breaking of the bonds between carbon atoms within the hexagons, SWCNT models were developed to include surface reconstruction and the formation of new groups. The SWCNT models are open-ended with up to 160 atoms, and the dangling bonds on carbon atoms are saturated with hydrogen. A CNT that is four hexagons long is sufficient to model the structure of a SWCNT, because the attached groups do not affect the structure outside of this area. Several models of SWCNTs were considered, including (9,0) metallic, (7,0), (8,0) semiconducting zigzag, and (5,5), (6,6), (7,7), (8,8) metallic armchair structures with lengths of about 12 Å to study the dependence of the oxidation processes on the SWCNT chirality and diameter. In order to simulate an infinite SWCNT, the positions of the atoms at the edges are fixed when the geometry of the structures is optimized.

4. Results

4.1 High-resolution electron microscopy

All O-MWCNTs were examined by HR-TEM to verify the morphology of the material. Several details of the functionalised sample were noted. First, a small amount of amorphous carbon was observed in all oxidized samples. The HR-TEM micrograph (Figure 1) illustrates possible disorder on the outer walls of the MWCNTs.
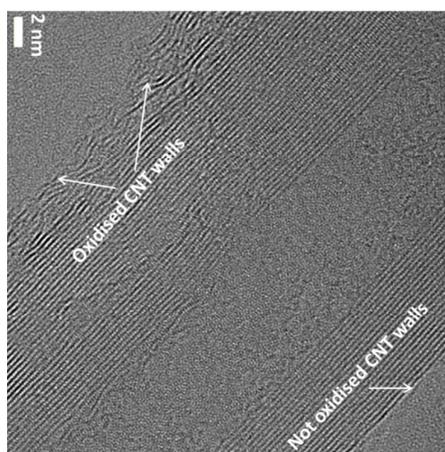

Figure 1.HR-TEM micrograph of an oxidized MWCNT.

Depending on the oxidation protocol, some changes in the ratios of the different types of disorder appeared. After the sonication process, the CNT walls were more exfoliated than after reflux treatment. Reflux causes some MWCNT walls to unroll (see supporting information).

4.2 Raman spectroscopy

Raman spectroscopy allows the quantitative estimation of the amount of amorphous carbon and of structural disorder on the outer walls of the CNTs. For O-MWCNTs, two Raman peaks are considered to estimate their quality: 1) the tangential stretching G-mode, which is usually located between 1500 and 1600 cm^{-1} and corresponds to the tangential in-plane stretching vibrations of the C-C bonds within the graphene structure, and 2) the double resonance D-mode (1350 cm^{-1}), which is usually related to disorder within the MWCNT structure [20]. The parameter commonly used to quantitatively estimate the amount of disorder in a hexagonal graphite-like structure like that of the MWCNTs is the ratio of the D and G peak intensities, called the R factor ($R=I_D/I_G$). According to the Raman spectra, the shorter O-MWCNTs are more damaged (Figure 2A). The same tendency was observed for all oxidized samples, although the amount of disorder is different depending on the oxidation treatment (Figure 2B). Among all three oxidation methods discussed, sonication in a highly oxidizing acid mixture causes the most damage to the MWCNT structure.
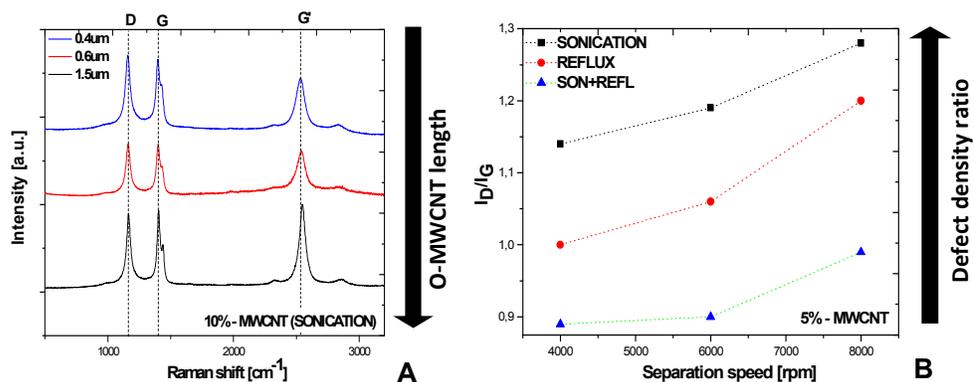

Figure 2.(A) Raman spectra for O-MWCNTs with different lengths and (B) defect density ratios for O-MWCNTs with different lengths fabricated using different oxidation protocols.

4.3 FTIR

The molecular groups attached to the MWCNT walls during the chemical treatment were identified by FTIR. Figure 3A compares the absorption spectra of 2%-MWCNTs for the entire synthesized sample and for the fraction with a mean length of 0.5 μm treated according to the three different protocols. Figure 3B presents the IR spectra of 10%-MWCNTs of three different lengths sonicated in acid solution. A strong dependence of the structure on the oxidation method and CNT size is found. The intensities of peaks IV (at 1630 cm^{-1}) [21, 22, 23] and V (at 1575 cm^{-1}) assigned to a stretching mode of C=C of aromatic groups depend on both these factors. Peak III, which is related to C=O stretching in COOH groups, is observed at around 1715 cm^{-1} for sonicated (protocol I) or refluxed (protocol II) MWCNTs but is shifted to around 1730 cm^{-1} for the sample subjected to both sonication and reflux (protocol III). This indicates a higher quantity of carboxyl groups in the first two samples [24], which facilitates the formation of hydrogen bonds between COOH groups. Absorption peak VII at around 1385 cm^{-1}, which is ascribed to CH bonding in COH groups, shows up only for sonicated MWCNTs.
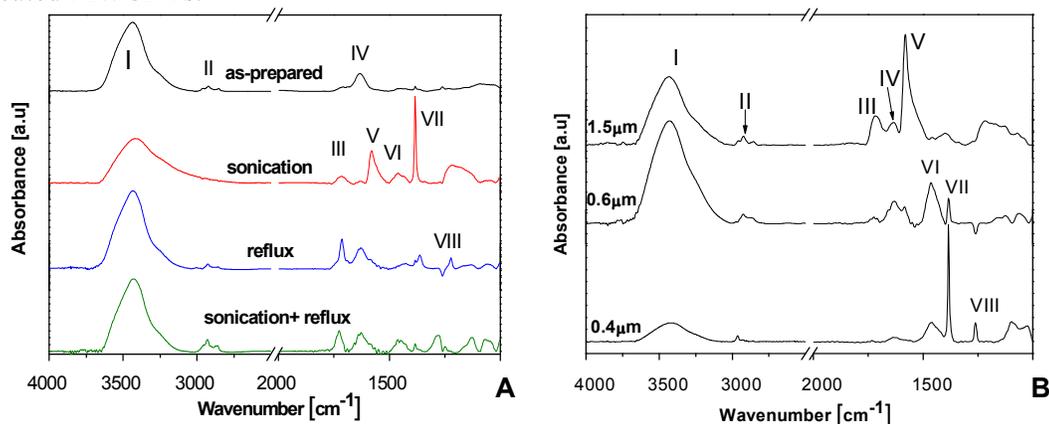

Figure 3.(A) Infrared absorption spectra of 2%-MWCNTs for the entire prepared sample and for the fraction with a mean length of 0.5 μm oxidized using the three different protocols. (B) Infrared absorption spectra of 10%-MWCNTs for the fractions with mean lengths of 0.4, 0.6, and 1.2 μm, sonicated for 3 h in H$_2$SO$_4$/HNO$_3$ solution. The roman numerals denote the following vibrations: (I) OH stretching, (II) CH$_3$ symmetric and asymmetric stretching, (III) C=O stretching, (IV,V) C=C stretching of aromatic cores on CNTs, (VI) CH$_3$ asymmetric stretching, (VII) CH bending vibration in aldehyde groups, and (VIII) CO stretching within carboxyl groups.

Both Raman and FTIR results indicate that protocol I is the most effective method of oxidation. The focused mechanical stress imposed on the sample in the acid solutions during sonication causes more damage to the graphite structure than the thermal energy supplied to the system in the reflux technique. The influence of the reflux time on the MWCNT structure is shown in Figure 4. With increasing treatment time, the intensity of absorption band IV at 1630 cm^{-1} decreases, whereas the peak at 1715 cm^{-1} becomes more pronounced. This suggests the progressive destruction of the graphite-like structure as the oxidation time increases. The reflux time of 15 minutes applied in protocols II and III is not sufficient to obtain well-oxidized MWCNTs.
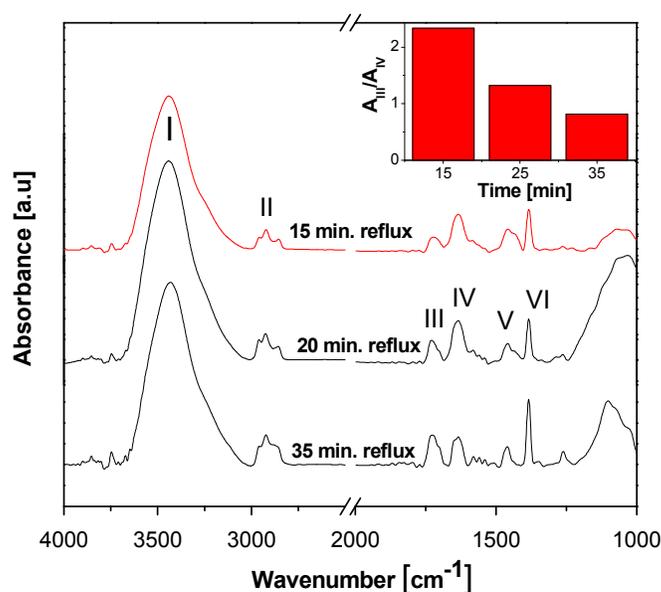

Figure 4.**Infrared absorption spectra of 5%-MWCNTs oxidized by reflux treatment for different times. The roman numerals denote the following vibrations [22]: (I) OH stretching, (II) CH$_3$ symmetric stretching, (III) C=O stretching, (IV,V) C=C stretching of aromatic cores on CNTs, (V) CH stretching within carbonyl groups, and (VI) CO stretching within carboxyl group. The inset shows the ratio of the integrated absorbance of bands III and IV as a function of treatment time.**

5. Computational results

To study in detail the processes occurring on the outer walls of the CNTs during oxidation treatment, first-principles calculations were conducted to determine the energies of vacancy formation and bond breaking. The attachment of the functional groups on the surfaces of the MWCNTs observed by FTIR (Figures 3 and 4) is also demonstrated. Based on the minimum

energy principle, the results reveal the most plausible reaction paths for attaching carbonyl and carboxyl functional groups to the sidewalls of CNTs. Figure 5 presents the energies needed for a SWCNT to undergo the transformations discussed below.
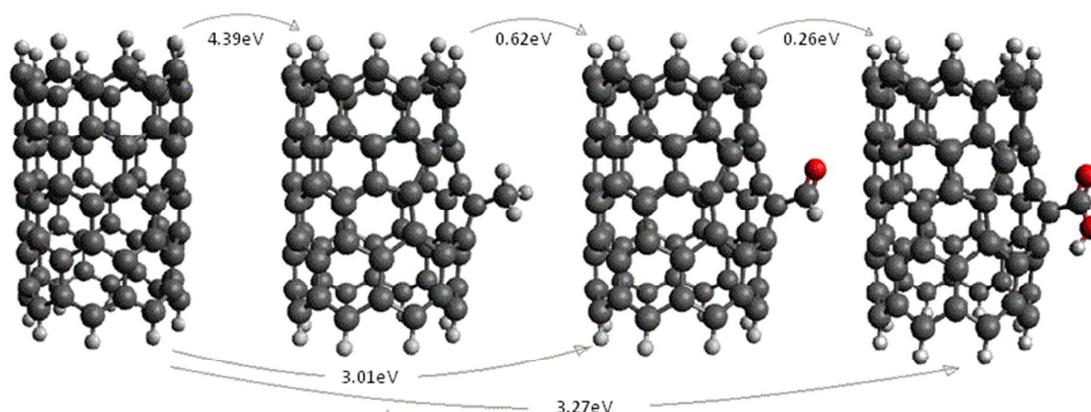

Figure 5.Process for the formation of carboxyl group on an (8,0) SWCNT.

Considering the acids used during the functionalization (nitric and sulphuric), the environment surrounding the CNT is rich in hydrogen ions and oxygen but lacks the carbon needed to form the observed functional groups. Consequently, the carbon atoms must come from the CNTs, either through destruction of the bonds within a hexagon and rehybridization of the free bonds or from CH_3 groups previously attached during the CVD synthesis (Figure 3-4). A methyl group can also be created during an oxidation treatment. Three dangling bonds to carbon atoms appear when a hexagon in the outer wall of a CNT is destroyed. One of the bonds is saturated with hydrogen ions from the surroundings, and the remaining ones create a double covalent bond to form a pentagon on the surface. A similar process takes place during vacancy formation [25]. In the following step, two hydrogen atoms are exchanged with an oxygen as an energetically favoured reaction. The remaining hydrogen atom can be replaced with a hydroxyl group, which completes the formation of a carboxyl group on the sidewall of a SWCNT. The energies of formation of various functional groups or defects depend on the chirality of the outer wall of the MWCNT (see Table 1). Less energy is needed to attach a given functional group to a metallic (8,8) CNT than is needed for a semiconducting (8,0) CNT. The same tendency is observed for the energy necessary to destroy two bonds within the graphene-like structure in a CNT: a semiconducting (8,0) CNT requires more energy to break bonds than a metallic CNT.

Table 1.Energies of formation of defects and functional groups on the surface of a SWCNT.

Energy of formation (E), eV		CNT (8,0) Semiconducting	CNT (9,0) Metallic	CNT (8,8) Metallic
E(vacancies)		4.70	4.32	4.18
E(pentagons)		0.69	0.62	-0.83*
E(CH3)		4.39	3.94	1.60
E(O=C-H)		3.01	2.41	1.46
E(COOH)		3.27	2.61	1.37
Energy needed to destroy two bonds		3.14	2.88	2.79
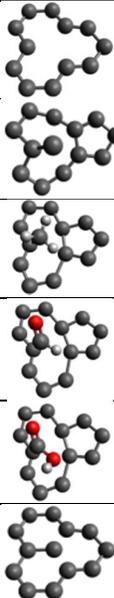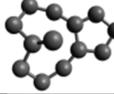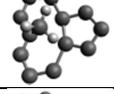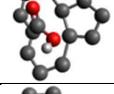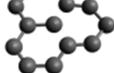
* Relaxation of the structure after the pentagon is formed makes this reaction exothermic for such a reactive metallic SWCNT.

The dependence of the partial binding energy between a SWCNT and a functional group on the total number of attached groups was analysed using the following formula:

$$\Delta E_n = \frac{E_{SWCNT+(FG)_n} - E_{SWCNT}}{n},$$

where $E_{SWCNT+(FG)_n}$ is energy of a SWCNT with n functional groups attached and E_{SWCNT} denotes the energy of a pristine CNT. Figure-6 shows the results for various types of SWCNTs.

The partial energy decreases with the number of attached functional groups. Every new functional group attached on a surface requires the breakage of two bonds between carbon atoms. This leads to a loss in the overall stiffness of the structure, and consequently less energy is needed to break additional bonds.

Moreover, the dependence of the bonding energies between the SWCNTs and the functional groups on the diameter and type of the SWCNT is studied. In particular, armchair-type SWCNTs, being metallic and hence more reactive, need considerably less energy to attach functional groups and to reconstruct the surface, in comparison to zigzag-type semiconducting CNTs.
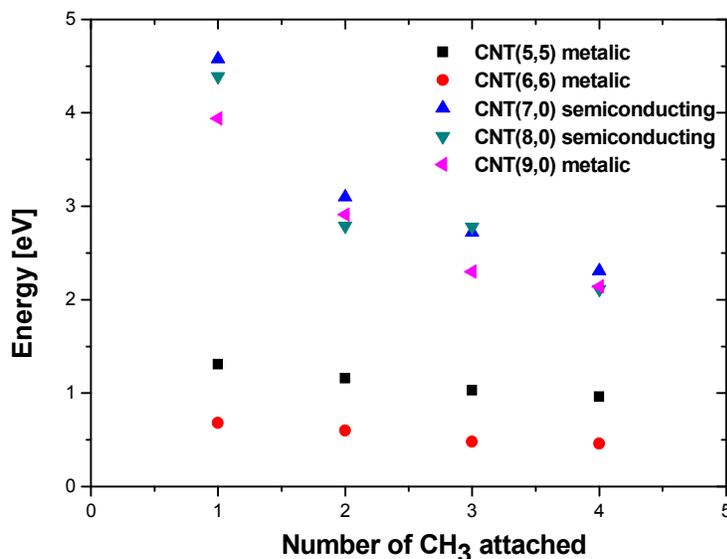
Figure 6.Dependence of the partial binding energy on the number of functional groups attached to the surface of a SWCNT.

6. **Conclusions**

The influence of three different oxidation protocols, 24 h of sonication (I), 15 minutes of reflux (II), and 3 h of sonication plus 15 minutes of reflux (III), on the outer walls of MWCNTs was studied by HR-TEM, Raman spectroscopy, Fourier transform infrared spectroscopy, and *ab initio* computational methods. The following conclusions are drawn:

- The oxidation treatment and CNT size strongly affect the degree of damage of the MWCNT walls. Sonication of MWCNTs is the most effective oxidation method among the three discussed.

- Based on *ab initio* calculations, the mechanism for the formation of carboxyl groups on the side walls of MWCNTs is proposed. In particular, CH_3 moieties (formed during the synthesis or oxidation process) are converted to COH groups and then COOH groups.

- The dependence of the bonding energy on the number of functional groups formed on a surface is established for CNTs with different chiralities.

Acknowledgements

References

[1] Ji S, Liu C, Zhang B, Yang F, Xu J, Long J, et al. Carbon nanotubes in cancer diagnosis and therapy. Biochim Biophys Acta 2010;1806(1):29–35.

[2] Kis A, Zettl A. Nanomechanics of carbon nanotubes. Philos Trans. A Mat Phys Eng Sci 2008;366(1870):1591–1611.

[3] Janas D, Koziol KK. Rapid electrothermal response of high-temperature carbon nanotube film heaters. Carbon 2013;59:457-463.

[4] Kostarelos K, Bianco A, Prato M. Nature Nanotechnol 2009;4:627-32.

[5] Chen J, Hamon A, Hu H, Chen Y, Rao AM, Eklund PC, et al. J.Phys.Chem.1998;282:95-8.

[6] Datsyuk V, Kalyva M, Papagelis K, Parthenios J, Tasis D, Siokou A, et al. Chemical oxidation of multiwalled carbon nanotubes. Carbon 2008;46(6):833–40.

[7] Liu J, Rinzler AG, Dai H, Hafner JH, Bradley RK, Boul PJ, et al. Fullerene Pipes. Science 1998;280:1253-6.

[8] Chełmecka E, Pasterny K, Kupka T, Stobiński L. DFT studies of COOH tip-functionalized zigzag and armchair single wall carbon nanotubes. J Mol Model 2012;18(5):2241–6.

[9] Veloso MV, Filho AGS, Filho JM, Fagan SB, Mota R. *Ab initio* study of covalently functionalized carbon nanotubes. Chem Phys Lett 2006;430:71–4.

[10] Kar T, Akdim B, Duan X, Pachter R. Open-ended modified single-wall carbon nanotubes: A theoretical study of the effects of purification. Chem Phys Lett. 2006;423:126–30.

[11] Hohenberg P, Kohn W. Inhomegeneous Electron Gas. Phys Rev. 1964;136:864B.

[12] Kar T, Scheiner S, Roy AK. The effect on acidity of size and shape of carboxylated single-wall carbon nanotubes. A DFT-SLDB study. Chem Phys Lett. 2008;460:225–9.

[13] Wongchoosuk C, Udomvech A, Kerdcharoen T. The geometrical and electronic structures of open-end fully functionalized single-walled carbon nanotubes. Curr Appl Phys 2009;9:352–58.

[14] Frisch MJ, Trucks GW, Schlegel HB, Scuseria GE, Robb MA, Cheeseman JR, et al. Gaussian 09, Revision **D.01**, Wallingford CT: Gaussian, Inc.; 2009.

[15] Becke AD. Density-Functional Exchange-Energy Approximation with Correct Asymptotic Behavior. J Chem Phys 1994;98:5648-52.

[16] Lee C, Yang W, Parr RG. Development of the Colle-Salvetti correlation-energy formula into a functional of the electron density. Phys Rev. B 1988;37:785-9.

[17] Stephens PJ, Devlin FJ, Chabalowski CF, Frisch MJ. Ab initio calculation of vibrational absorption and circular dichroism spectra using density functional force fields. J Phys Chem 1994;98:11623-7.

[18] Gonze X, Amadon B, Anglade PM, Beuken JM, Bottin F, Boulanger P, et al. Comput Phys Commun 2009 ;180:2582-615.

[19] Gonze X, Rignanese GM, Verstraete M, Beuken JM, Pouillon Y, Caracas R, et al. ABINIT: First-principles approach to material and nanosystem properties. Zeit Kristallogr 2005;220:558-62.

[20] Lehman JH, Terrones M, Mansfield M, Hurst KE, Meunier V. Evaluating the characteristics of multiwall carbon nanotubes. Carbon 2011;49: 2581–2602.

[21] Socrates G. Infrared and Raman characteristic group frequencies. Tables and Charts. 3rd ed. New York: Wiley; 2001.

[22] J. Senthilnathan , K. Sanjeeva Rao and M. Yoshimura, Submerged liquid plasma – low energy synthesis of nitrogen-doped graphene for electrochemical applications, J. Mater. Chem. A,2014, 2, 3332-3337.

[23] F. Yang, M. Zhao, B. Zheng, D. Xiao, Li Wu,Y. Guo Influence of pH on the Fluorescence Properties of Graphene Quantum Dots Using Ozonation Pre-oxide Hydrothermal Synthesis. J. Mater. Chem., 2012, 22, 25471–25479. (see Supporting Information).

[24] Zhang J, Zou H, Qing Q, Li Q, Liu Z, Gou X, et al. Effect of chemical oxidation on the structure of single walled-carbon nanotubes. J Phys Chem B 2003;107:3712-8.

[25] Rossato J, Baierle RJ, Fazzio A, Mota R. Vacancy formation process in carbon nanotubes: First-principles approach. Nano Lett 2005;5:197-200.

OXIDATION MECHANISM OF MULTIWALLED CARBON NANOTUBES